Journal of Sound and Vibration 642 (2026) 119948

Contents lists available at ScienceDirect

Journal of Sound and Vibration

journal homepage: www.elsevier.com/locate/jsvi

Rapid Communications

A simple phase synchronization algorithm for aeroacoustics studies of multi propeller system

Mansi Bhardwaj [a,*], Tze Pei Chong [a], Paruchuri Chaitanya [b], Phillip Joseph [b,1]

[a] Department of Mechanical and Aerospace Engineering, Brunel University of London, Uxbridge, UB8 3PH, United Kingdom
[b] Institute of Sound and Vibration Research, University of Southampton, Southampton, SO17 1BJ, United Kingdom

ARTICLE INFO

Keywords:
Dual propeller
Co-rotating
Synchronized propellers
Synchronization logic
Noise decomposition
Gaussian filter
Noise filter algorithm

ABSTRACT

Phase synchronization between propellers is a critical factor influencing aerodynamic interactions and their noise generation in electric vertical take-off and landing (eVTOL) vehicles and unmanned aerial systems (UAS). While several studies have demonstrated the benefits of phase control of propellers for noise reduction purposes, practical methods for accurately identifying phase differences in experimental environments are complicated and remain limited. This paper introduces a phase detection and filtering algorithm utilizing Gaussian weighting technique to extract data corresponding to the required phase differences between two propellers. It also assists in decomposing the noise into different angular positions. The algorithm compares the timing signals from two tachometers and separates the target data according to the defined phase difference between the propellers. If both the flow and noise fields are measured simultaneously, both data can then be decomposed based on the defined phase difference and the angular position of the propellers. Validation results confirm the reliability of this method in separating the datasets into defined phase difference with good accuracy, facilitating the systematic analysis of tonal noise behavior in synchronized propeller configurations.

1. Introduction

The rapid development of urban air mobility (UAM) concepts and electric vertical take-off and landing (eVTOL) vehicles has renewed interest in the aeroacoustics performance of multi-rotor systems. Although multi-rotor systems increase the efficiency of the propulsion system, use of multiple propellers in a small space can increase the overall level of noise radiation. An important question arises with regard to the tonal noise behavior due to the presence of multiple propellers. Studies have shown that the relative positioning of the blades of adjacent propellers play a vital role in controlling the noise generation, which is governed by the constructive or destructive interference of their periodic loading noise [1].

Previous studies have demonstrated that adjusting phase differences between propellers can significantly reduce tonal noise at the fundamental and harmonics of blade passing frequency (BPF) [2]. For example, Schiller *et al.* [3] and Pascioni *et al.* [4] showed that phase synchronization of distributed rotors could suppress tonal components by mitigating unsteady blade loading. The underlying physical mechanisms and the noise reduction through synchrophasing has been investigated in detail by Joseph et al. [5], demonstrating how controlling the relative phase angles between the propellers influence tonal interference patterns. Shao *et al.* [6] and

* Corresponding author.
E-mail address: mansi.bhardwaj@brunel.ac.uk (M. Bhardwaj).

[1] Given his role as Subject Editor, Phillip Joseph had no involvement in the peer-review of this article and has no access to information regarding its peer-review. Full responsibility for the editorial process for this article was delegated to another journal editor.

https://doi.org/10.1016/j.jsv.2026.119948
Received 28 January 2026; Received in revised form 19 May 2026; Accepted 5 June 2026
Available online 7 June 2026

Welker [7] discussed aerodynamic interaction effects due to phase synchronization of the propellers. More recently, Del Duchetto *et al.* [8] demonstrated that phase synchronization can achieve robust noise reduction not only in hovering but also during forward flight.

Most published studies on the aeroacoustics of multiple propellers, including those cited above, rely on achieving propeller synchronization *a priori*. In practice, however, synchronization presents two major challenges. First, all propeller motors must maintain identical speeds at all times, which requires continuous feedback control to compensate for disturbances and load variations. Second, even with accurate speed regulation, small differences in motor dynamics can lead to gradual phase drift, making long-duration data acquisition difficult. Existing approaches for phase control typically depend on costly hardware and complex control systems, limiting their suitability for flexible laboratory experiments. Consequently, the practical challenges of enforcing or extracting controlled phase differences in experimental settings remain persistent.

To address these challenges, this paper proposes a phase synchronization algorithm tailored for aeroacoustics studies of multiple propellers. The algorithm has been shown to accurately detect the instantaneous phase difference between two unsynchronized propellers, which naturally vary over time. This algorithm is a post processing method, which uses sufficient noise dataset, typically acquired over minutes and recorded together with the corresponding tachometer signals. These tachometer signals are then used to reconstruct the instantaneous phase difference between the two propellers, which allows the mapping of the acoustic response, particularly the tonal noise components, against the continuously changing phase angles. This enables systematic investigation of propeller-propeller interaction effects without requiring physical phase control systems. The validity of the algorithm has been verified by comparing its results against measurements obtained with electrically phase-synchronized propeller system, demonstrating its reliability as a practical and flexible alternative for laboratory studies.

2. Methodology

2.1. Experimental setup

The experiments were conducted in an aeroacoustics facility at Brunel University of London. For the acoustic measurements, a single G.R.A.S 46AE free-field condenser microphone was used. Calibration of this microphone was performed using a G.R.A.S 42AB sound calibrator. Microphone was positioned in the propeller plane at a distance of 1.2 m from the center between the two propellers. A representation of the setup is shown in Fig. 1(a). The noise data in this study is presented in terms of Sound Pressure Level (SPL), with a reference pressure set at 20 μPa.

As shown in Fig. 1(a), the phase angle of the master propeller relative to the datum, with positive achieved in the clockwise rotation, is defined as θ_1. Note that the angular orientation of the master propeller, ϕ, which will be discussed in Section 2.2, is equivalent to the master propeller phase angle θ_1 (i.e. $\phi \equiv \theta_1$). On the other hand, the phase angle of the slave propeller relative to the datum, which is not necessary the same value as that of the master propeller, is defined as θ_2. The phase angle difference between the two propellers is therefore:

$$\Delta\theta = \theta_2 - \theta_1. \tag{1}$$

Fig. 1(b) contains a table showing the different combinations of θ_1, θ_2, and $\Delta\theta$ investigated in this study.

The motor controllers driving the propellers were operated in two modes: synchronized and unsynchronized. For both operating modes, the propellers were run at 3000 and 4000 rpm in a co-rotating configuration. The same sampling frequency of 100 kHz was maintained across both cases. In the unsynchronized mode, the system was operated for a sufficient duration (5 minutes in the current setup) to acquire a dataset suitable for phase analysis, which was subsequently processed using the proposed synchronization algorithm. The electronically synchronized mode was then employed to repeat the experiment and validate the algorithm's performance. Details of both setups are provided in the following subsections.

2.1.1. Electronic synchronization system

The experimental rig consisted of two identical propeller-motor assemblies mounted side-by-side on an aluminum profile frame. Each assembly comprised a brushless DC motor (T-Motor) fitted with an APC 11 × 4.7 in. propeller, an optical encoder attached to the motor shaft, a programmable electronic speed controller to regulate propeller speed, a DC power supply, and a tachometer sensor to record blade-passage trigger points for verification of the phase difference.

Phase synchronization between the two propellers is achieved using a microcontroller implementing a Proportional-Integral-Derivative (PID) control algorithm:

$$u = K_p e + K_i \int e\,dt + K_\mathrm{d} \frac{d}{dt} e. \tag{2}$$

The control logic continuously captures the angular position of the master (reference) propeller and minimize the error between the master and slave (second) propeller positions. A flow chart describing the PID logic is shown in Fig. 1(c).

The PID gains (K_p, K_i, K_d) were adjusted to provide the appropriate output response for the response time, t, and to reduce the error, e, between the required and actual position of the propeller. The proportional term ($K_p e$) is used to correct the instantaneous phase error, the integral term ($K_i \int e\,dt$) removes the steady-state error, and the derivative term ($K_\mathrm{d} \frac{d}{dt} e$) introduces damping to suppress oscillations in signals. The resulting output is given as an RPM correction to the slave propeller.

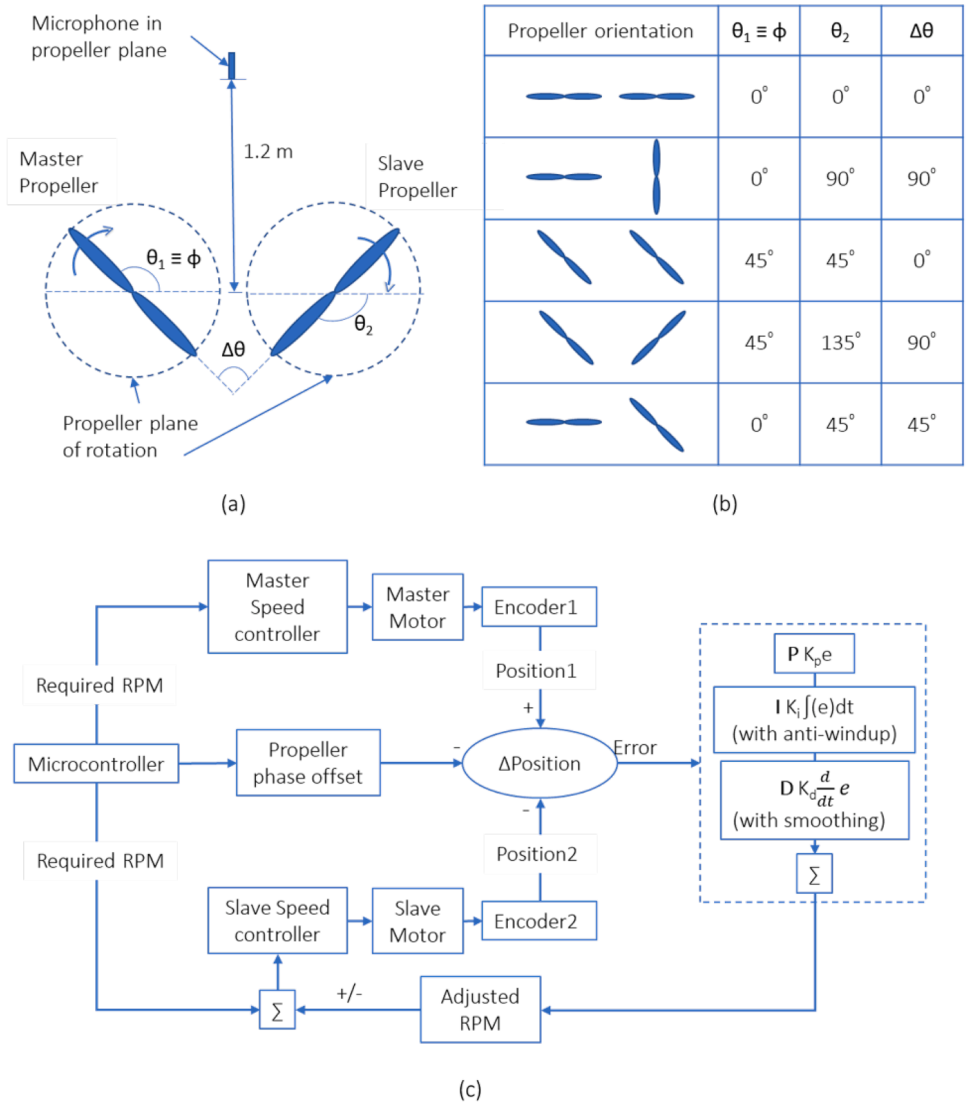

Fig. 1. (a) Top-view schematic of the experimental setup showing the propellers rotating plane, (b) Table showing examples of the propeller phase angles (θ_1, θ_2) and phase difference ($\Delta\theta$) investigated in this study, and (c) Control architecture for propeller synchronization using a PID controller.

2.1.2. Algorithm-based synchronization

The experimental setup is similar to the electronic synchronization system discussed above, with the key difference being that the two propellers were not synchronized physically. Instead, sufficient unsynchronized data was processed using the data filter algorithm to be discussed in Section 2.2, with the tachometer readings serving as the input for phase detection.

2.2. Phase filtering algorithm

After acquiring data in the unsynchronised mode, post-processing begins by reconstructing the instantaneous phase angle of each propeller, θ_1 and θ_2, from their respective tachometer signals. For each propeller, the phase angle is obtained from the elapsed time since the previous tachometer trigger, normalised by the instantaneous rotation period, according to

$$\theta_1(t) = \frac{t - t_{1,k}}{t_{1,k+1} - t_{1,k}} \times 360 \text{ (deg)}, \quad \theta_2(t) = \frac{t - t_{2,k}}{t_{2,k+1} - t_{2,k}} \times 360 \text{ (deg)}, \tag{3}$$

where $t_{1,k}$ and $t_{2,k}$ denote consecutive tachometer trigger times for the master and slave propellers, respectively, and t denotes the instantenous time of the experiment. To enable a direct comparison between the two propellers, the instantaneous phase angles are linearly interpolated onto a common time base corresponding to the acoustic sampling timeline. A fixed time offset is applied to account for the difference in acoustic propagation time from each propeller to the measurement location. This procedure maps each acoustic data sample to a relative inter-propeller phase difference, $\Delta\theta$ (Eq. 1)

The minimum filtering window length was kept constant across all datasets and chosen to span a sufficient number of blade-passing periods to ensure consistent capture of the radiated acoustic energy. This ensures that variations in record length do not influence the comparison between different cases.

To facilitate the filtering process, Gaussian weighting filter is incorporated into the algorithm, combining two main conditions:

1. Phase Difference Weighting (ω_θ): With the angular offset between the two propellers denoted as $\Delta\theta$, this weighting ensures that only data corresponding to a specific offset $\Delta\theta_{\text{target}}$ are considered:

$$\omega_\theta = \exp\left[-\frac{1}{2}\left(\frac{\Delta\theta - \Delta\theta_{\text{target}}}{\sigma_\theta}\right)^2\right] \tag{4}$$

where σ_θ represents the filter tolerances ranges for the propeller phase difference.

2. Angular Orientation Weighting (ω_ϕ): This weighting selects data corresponding to instances when the master propeller is at a specific angular orientation (ϕ_{target}) relative to its reference position (see Fig. 1a). Note that ϕ is only applicable to the master propeller and is equivalent to θ_1.

$$\omega_\phi = \exp\left[-\frac{1}{2}\left(\frac{\phi - \phi_{\text{target}}}{\sigma_\phi}\right)^2\right] \tag{5}$$

where σ_ϕ defines the filter tolerances ranges for the propeller orientation. When the noise is decomposed into individual angular positions, noise data is acquired within the targeted orientation range (σ_ϕ). By contrast, when noise decomposition is not required, σ_ϕ is set to 360°. This implies that all the angular positions are included in the synchronization study.

The combined weighting is expressed as:

$$\omega = \omega_\theta \ \mathbf{x} \ \omega_\phi. \tag{6}$$

This weighting factor is used exclusively to identify continuous data segments that correspond to the desired phase difference and angular position, if applicable. For each identified segment, the power spectral density (PSD) is computed using Welch's method with a Hamming window. The resulting PSDs are subsequently averaged to obtain the mean spectrum, thereby achieving effective phase control via phase-averaging of the acoustic measurements, and potentially the flow field data, if acquired simultaneously.

In the current study, the electronically synchronized setup maintained the propeller speed within approximately ±5 RPM of the target operating condition. On the other hand, the unsynchronized setup exhibited transient RPM fluctuations of up to approximately ±50 RPM, though the propellers typically returned to the desired speed within a few revolutions. Such fluctuations could potentially generate very short noise data segment and are therefore excluded during the filtering process. To maintain a fair comparison between the electronically and algorithmically synchronized configurations, the filter tolerance range, σ_θ was typically set to 5°. This provides a sufficiently narrow phase selection while still retaining enough valid data segments for reliable spectral averaging.

3. Results

3.1. Validation of filtering algorithm

The algorithm was validated by comparing the noise spectra obtained from the electronically synchronized propellers against those generated via the algorithmic synchronization. Fig. 2(a) compares the noise spectra for both synchronization methods at $\Delta\theta = 0°$ for propellers operating at 4000 RPM. The spectrum obtained from the unsynchronized system is also included as a baseline. Note that the noise spectra representing algorithmic synchronization are reconstructed from the unsynchronized raw acoustic data via the post-processing phase filtering method described previously.

The noise spectra of the electronic and algorithmic synchronization methods are in excellent agreement, capturing both tonal and broadband features across the entire frequency range. While the noise spectrum of the baseline unsynchronized propellers largely follows a similar trend, noticeable differences in the sound pressure level are observed at the fundamental blade pass frequency tone, as highlighted in the inset of Fig. 2(a), and its higher-order harmonics.

Two primary conclusions can be drawn from Fig. 2(a). First, applying a phase-filtering algorithm with Gaussian weighting to acoustic data from unsynchronized operation accurately reconstructs the acoustic signatures of a physically synchronized setup. Second, propellers operating synchronously with a fixed phase difference ($\Delta\theta$) exhibit distinct acoustic characteristics compared to their unsynchronized counterparts. This highlights a critical phenomenon: when two propellers operate in close proximity, their acoustic fields interfere either constructively or destructively depending on their relative phase angle, a behavior well-documented in the literature.

To investigate the sensitivity of noise radiation to the relative propeller phase angle ($\Delta\theta$), Fig. 2(b) presents the band-passed overall sound pressure level (OASPL), integrated within ±15 Hz of the fundamental blade passage frequency at 3000 and 4000 RPM. Both the electronic and algorithmic synchronization methods exhibit highly consistent trends in the band-passed OASPL, with a maximum discrepancy of only approximately 0.6 dB, further confirming the reliability of the phase-filtering algorithm. The maximum band-passed OASPL occurs at $\Delta\theta = 0°$. As $\Delta\theta$ increases to 45°, the OASPL decreases marginally, followed by a sharper, more pronounced reduction as $\Delta\theta$ approaches 90°. This localized steepening of the negative gradient aligns with trends reported in previous studies [3–8].

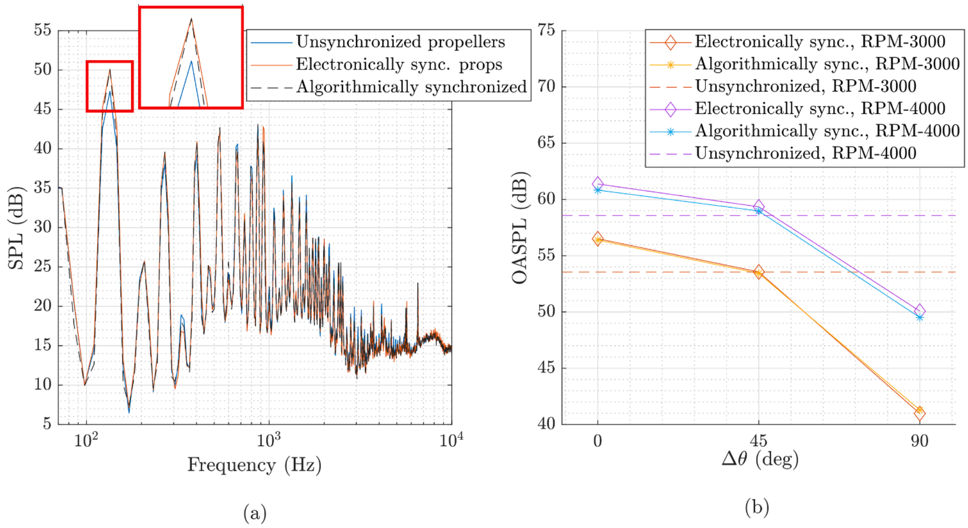

Fig. 2. (a) Comparison of noise spectra for unsynchronized propeller configuration, electronically synchronized propellers, and algorithmic synchronization at 4000 RPM and ($\Delta\theta = 0°$) (b) Variation of OASPL (by integrating PSD over the frequency band defined as BPF ±15 Hz) with relative phase difference ($\Delta\theta$) at 3000 and 4000 RPM for both the electronically synchronized propellers and algorithmic synchronization.

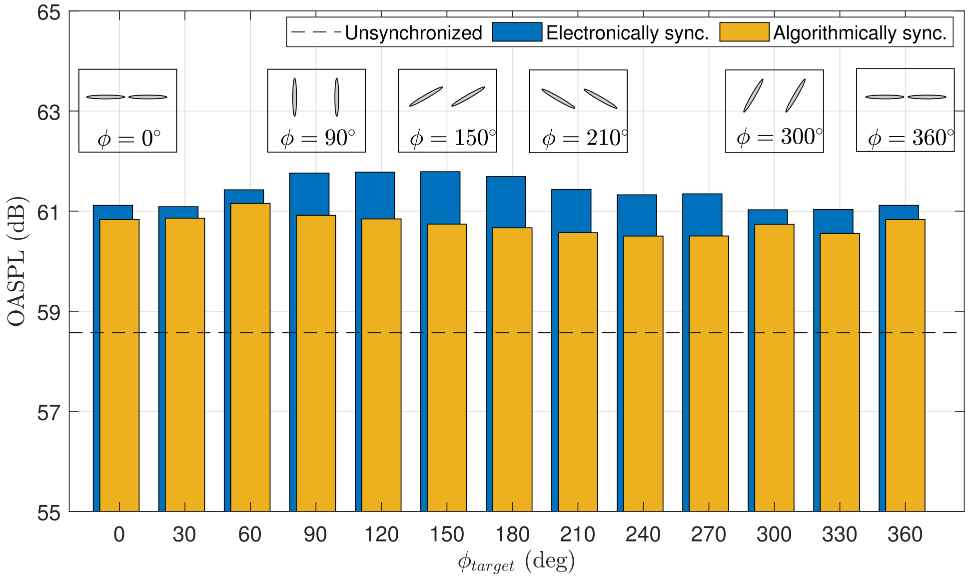

Fig. 3. Comparison of band-passed OASPL as a function of target propeller angular orientation (ϕ_{target}) for electronically and algorithmically synchronized configurations. The data are integrated within ±15 Hz of the fundamental blade passage frequency for a fixed relative phase difference of $\Delta\theta = 0°$ at 4000 RPM. The horizontal dashed line denotes the baseline band-passed OASPL for the unsynchronized configuration. Representative schematics illustrating the twin-propeller orientations at selected angular positions (ϕ) are provided at the top.

3.2. Noise decomposition

By performing spectral analysis of the raw acoustic data from the unsynchronized propellers using the classical fourier transform technique, one can only obtain the overall spectral energy distribution and time-averaged tonal components. This approach lacks the resolution to distinguish individual propeller contributions or resolve specific phase relationships. Consequently, even under a fixed relative phase, $\Delta\theta$, it is difficult to isolate the noise level associated with the fundamental blade pass frequency as a function of an individual blade's angular position ϕ (or θ_1, see Fig. 1a).

By employing the current algorithmic synchronization technique, the acoustic field of unsynchronized propellers can be decomposed to resolve specific noise levels as a function of the blade angular orientation ϕ. Fig. 3 illustrates the band-passed OASPL associated with the fundamental blade pass frequency at $\Delta\theta = 0°$, 4000 RPM across various target angular positions (ϕ_{target}). For this analysis, σ_ϕ is set to 15° (refer to Eq. 5), establishing a 15° sampling window for each (ϕ_{target}). Schematic drawings of selected propeller orientations are included at the top of the figure for visual clarity. Note that the tip-to-tip clearance between adjacent propellers is $0.02D$, where D denotes the propeller diameter.

The figure demonstrates that the synchronized band-passed OASPL exhibits a weak dependence on the target angular orientation (ϕ_{target}). For both the electronically and algorithmically synchronized configurations, systematic variations in the band-passed OASPL are observed across the investigated angles, with fluctuations remaining within a narrow range of approximately 1 dB. While the electronically synchronized setup consistently produces marginally higher OASPL values than the algorithmic approach, the energy-averaged OASPL across all orientation angles for both synchronization methods remains in close agreement with the corresponding total synchronized values presented in Fig. 2.

When the experimental campaign includes flow diagnostics, such as using hot-wire anemometry to measure unsteady velocity fluctuations, both acoustic and flow data can be synchronized and decomposed using the current method. This integrated approach provides a more comprehensive understanding of the flow-acoustic coupling, and enables the isolation and identification of aeroacoustics noise mechanisms associated with specific blade orientations.

3.3. Discussion of limitations

The filtering algorithm assumes that the propellers operate at a quasi-stationary rotational speed throughout the acquisition window. While effective, this approach presents several inherent limitations:

1. Because the algorithm relies on the coincidental occurrence of desired phase relationships, a significant portion of the raw data is discarded. Consequently, extended acquisition periods are required to compile a statistically significant sample set.
2. The accuracy of the synchronization diminishes in low signal-to-noise ratio environments, where the tonal noise signature is difficult to distinguish from background broadband noise or measurement interference.
3. The sampling rate of the tachometer system dictates the precision of the tracked rotational speed. At high RPMs for the propellers, insufficient sampling can limit the angular resolution, potentially introducing errors into the phase-locking process.

Despite these constraints, the proposed algorithmic synchronization remains a highly cost-effective and flexible alternative to complex and expensive hardware-based systems. Its ease of implementation makes it particularly well-suited for diverse experimental aeroacoustics facilities where physical synchrophasing is not feasible.

4. Conclusions

This study introduces a novel algorithmic phase-synchronization technique for the aeroacoustics analysis of multi-propeller systems. Through rigorous validation against an electronically synchronized configuration, the proposed post-processing algorithm is demonstrated to accurately and reliably categorize unsynchronized datasets into discrete, phase-locked bins without significant loss of accuracy. The acoustic trends extracted using this method align closely with established literature. Specifically, the maximum noise radiation occurs when the relative phase angle between the two propellers is zero ($\Delta\theta = 0°$). As $\Delta\theta$ increases to 45°, the acoustic outputs of the synchronized and unsynchronized configurations become comparable. Conversely, pronounced noise mitigation is achieved when the propellers operate completely out of phase ($\Delta\theta = 90°$), demonstrating that a destructive acoustic interference field can be strategically applied through precise phase synchronization to achieve substantial noise reduction.

Furthermore, the capability of the algorithm to decompose the acoustic field into distinct propeller blade orientations (ϕ) has been successfully demonstrated. Although this paper only presented the noise decomposition of the $\Delta\theta = 0°$ configuration, the underlying methodology is inherently adaptable to non-zero relative phase differences,

Overall, the proposed algorithm offers a low-cost, robust, and versatile approach for resolving phase-locked characteristics in experimental environments where hardware-based synchronization is not feasible or unavailable. By enabling the isolated decomposition of noise radiation at specific angular positions, this methodology provides deeper insights into the influence of blade orientation on noise generation. This methodology enables a highly detailed analysis of propeller-propeller aerodynamic interactions and the resulting acoustic field, ultimately offering a valuable tool for the aeroacoustics optimization of future multi-rotor systems.

CRediT authorship contribution statement

Mansi Bhardwaj: Writing – original draft, Validation, Software, Methodology, Investigation, Conceptualization; **Tze Pei Chong:** Writing – review & editing, Validation, Supervision, Methodology, Conceptualization; **Paruchuri Chaitanya:** Writing – review & editing, Software, Supervision, Conceptualization; **Phillip Joseph:** Writing – review & editing, Supervision, Conceptualization.

Data availability

Data will be made available on request.

Declaration of competing interest

The authors declare that they have no known competing financial interests or personal relationships that could have appeared to influence the work reported in this paper.

Acknowledgments

This research did not receive any specific grant from funding agencies in the public, commercial, or not-for-profit sectors.

References

[1] B.B. Turhan, Z. Yi, D. Rezgui, M. Azarpeyvand, Phase synchronization in noise control: advantages, limitations, and future perspectives, in: AIAA Aviation Forum and Ascend 2025, 2025, p. 3647.
[2] A. Zarri, F.d. Prenter, F. Avallone, D. Ragni, D. Casalino, Effects of phase synchronization on the tonal sound directivity of distributed propellers, J. Acoust. Soc. Am. 157 (5) (2025) 3267–3281.
[3] N.H. Schiller, K.A. Pascioni, N.S. Zawodny, Tonal noise control using rotor phase synchronization, in: Vertical Flight Society Annual Forum and Technology Display (VFS Forum 75), NF1676L-31452, 2019.
[4] K.A. Pascioni, S.A. Rizzi, N. Schiller, Noise reduction potential of phase control for distributed propulsion vehicles, in: Aiaa Scitech 2019 Forum, 2019, p. 1069.
[5] P. Joseph, P. Chaitanya, S. Elliott, M. Bhardwaj, T.P. Chong, Propeller tonal noise reductions through synchrophasing: mechanisms and performance, J. Sound Vib. 610 (2025) 119110.
[6] M. Shao, Y. Lu, X. Xu, S. Guan, J. Lu, Experimental study on noise reduction of multi-rotor by phase synchronization, J. Sound Vib. 539 (2022) 117199.
[7] N. Welker, D. Maynes, Aerodynamic effects of phase offset between synchronized propellers in hover (2023).
[8] F. Del Duchetto, T. Pagliaroli, P. Candeloro, K.-S. Rossignol, J. Yin, Aeroacoustic study of synchronized rotors, Aerospace 12 (2) (2025) 162.